Research Article

Received: 6 March 2019 Revised: 4 June 2019 Accepted article published: 17 June 2019 Published online in Wiley Online Library: 22 July 2019

(wileyonlinelibrary.com) DOI 10.1002/jctb.6118

Control of specific growth rate for the enhanced production of human interferon α2b in glycoengineered *Pichia pastoris*: process analytical technology guided approach

Srikanth Katla,[a] Naresh Mohan,[a] Satya S Pavan,[a] Uttariya Pal[b] and Senthilkumar Sivaprakasam[a]*

Abstract

BACKGROUND: Process variability in bioprocess systems involving genetically engineered strains is a common bottleneck and a real-time insight of the on-going process is crucial to achieve the desired product and its quality. In this study, a process analytical technology (PAT) platform was developed for the monitoring and control of specific growth rate during methanol induction phase (μ_{met}) of glycoengineered *Pichia pastoris* fermentation for human interferon alpha 2b (huIFNα2b) production.

RESULTS: The PAT guided approach involves real-time monitoring of capacitance (ΔC) facilitating online estimation of specific growth rate (μ_{est}), which serves as a process input during controller application. Fed-batch experiments using pulsed-feeding of methanol at different dosage (20 g and 30 g) did not significantly influence μ_{met}. Exponential methanol feeding was achieved using a modified proportional, integral and derivative (PID) controller for different predefined specific growth rate set point (μ_{sp}) values, namely 0.015, 0.03, 0.04 and 0.06 h^{-1}. Exponential feeding strategy during the induction phase resulted in two crucial outcomes: (i) controlled methanol feeding rate (regulated by the developed PID controller) balanced the methanol consumption rate ($q_{s,met}$) of the *P. pastoris*; (ii) significant improvement in huIFNα2b titer (1483 mg L^{-1}) and specific productivity(>0.4 mg g^{-1}. h) was achieved by the robust control of μ_{met} at optimal (0.04 h^{-1}) value. The purified huIFNα2b was found to exhibit antiproliferative effect against human breast cancer cell lines.

CONCLUSIONS: Efficient control of μ_{met} at a very low narrow range was achieved with a long-term controller stability (>10 h) and the highest titer reported to date for huIFNα2b (at optimal μ_{met}) in the yeast expression platform.
© 2019 Society of Chemical Industry

Supporting information may be found in the online version of this article.

Keywords: process analytical technology; capacitance; glycoengineered *Pichia pastoris*; human interferon alpha 2b; specific growth rate estimator; PID controller; antiproliferative

INTRODUCTION

Human interferon alpha 2b (huIFNα2b) is a type I interferon with wide range of biological properties, namely antiviral, anti-proliferative and immunomodulatory.[1] In contrast to bacterial expression systems, *Pichia pastoris* (a methylotrophic yeast) has emerged as successful expression system for the production of various heterologous proteins, particularly biopharmaceuticals and industrial enzymes.[2–4] In our previous investigations, we have successfully expressed huIFNα2b having a potent N-glycosylation site in glycoengineered *Pichia pastoris* strain. This *Pichia pastoris* strain with engineered human type N-glycosylation can produce glycosylated huIFNα2b mimicking human type N-glycan moiety.[5,6]

Exploration of various genetic engineering strategies in the yeast expression system has opened up a clear understanding of the secretary pathway of protein processing and regulation of the traffic associated with its transport. This pathway channels the native unprocessed protein towards appropriate folding and post-translation modifications, followed by its secretion into the reaction broth. Introduction of stronger inducible promoters at the upstream of the heterologous protein sequence was attempted previously by aiming at higher recombinant product titers. Expression systems like *Pichia pastoris* had demonstrated their suitability as hosts for managing the excessive transcriptional load towards protein formation. Molecular engineering approaches, however

* *Correspondence to: S Sivaprakasam, Department of Biosciences and Bioengineering, Indian Institute of Technology Guwahati, Guwahati - 781039, Assam, India. E-mail: senthilkumar@iitg.ac.in*

a *BioPAT Laboratory, Department of Biosciences and Bioengineering, Indian Institute of Technology Guwahati, Guwahati, India*

b *Molecular Endocrinology Laboratory, Department of Biosciences and Bioengineering, Indian Institute of Technology Guwahati, Guwahati, India*

suffer from limitation of higher expression activity, which leads to the retention of improperly folded proteins in their endoplasmic reticulum (ER). Yeast overcame the stress due to higher expression rates by generating unfolded protein responses in their ER lumen.[7,8] Inappropriately/unfolded protein fractions in the culture supernatants demand extensive purification steps that would be strongly detract from the viable 'Quality by Design' perspective. Therefore, optimization of protein titer from *Pichia pastoris* could be achieved by developing the relationships between the various critical process parameters and product titers.

In eukaryotes especially yeast systems, a good relationship was observed between the specific growth rate (μ) of an organism and their respective protein productivities. Genome level expression studies on *Saccharomyces cerevisae* reveal that all the 268 genes and 13 transcription factors identified were dependent upon the specific growth rate for their activation.[9] The rates of transcription in such systems were highly dependent upon the μ values maintained. Cultivation of organisms carried out by manipulating μ was determined to have a stronger influence at their metabolic level. *Pichia pastoris* when operated at retentostat level, i.e. operating the organism at nearly zero specific growth rate ($\mu < 0.001\ h^{-1}$), lead to the transcriptional re-programming followed by the up-regulation of stress related genes and down-regulation of cell cycle machinery. This process strategy allocates less maintenance energy for cell turn over activities through lowest growth trajectories. For all growth associated products, it is well established that the proportionality constant is apparently conserved for typical μ and q_P (Specific productivity) values. This ratio represents the stoichiometric coefficient of the sequence of all pipeline events in the protein production machinery. Therefore, aiming to control μ (critical process parameter) at the process level will lead to a more promising product output.

Gaining real-time insight of the process leading to therapeutic protein production is crucial for enhanced process understanding and robust control of the undesired process perturbations.[10] Process analytical technology (PAT) tools play pivotal roles in maintaining the product quality and achieving maximum productivity through timely monitoring and control[11] of critical process parameters (CPPs). Moreover, bioprocess systems involving therapeutic protein production should embrace the PAT framework which is an initiative by the FDA (Food and Drug Administration) for ensuring consistent product quality.[12]

Dielectric spectroscopy has evolved as a promising PAT tool, for real-time monitoring and control of bioprocess systems. Non-invasive, *in situ* operations, selective measurement of viable biomass, simplified linear calibration and short interval measurements are salient features of dielectric spectroscopy.[13] The operational principle involves polarization of individual cell membranes by application of electric field where each cell acts as a tiny capacitor.[14] The measured signal (change in capacitance, ΔC or permittivity, ε) is a function of volume fraction of cells with intact membrane, thereby negating the quantification of dead cells.[15] Dielectric spectroscopy has been successfully employed for real-time monitoring of bacterial,[16] yeast,[17] filamentous fungi[18]and mammalian[19] cell populations. Studies addressing the feedback control of specific growth rate using mid-infrared (mid-IR), near-infrared (NIR), methanol sensor and calorimetry as a soft sensor[20–27] are highlighted in Table S1 of the Supporting Information. Only a few studies have successfully reported the capacitance-based monitoring and control of μ at a desired value for *Pichia pastoris* and *Penicillium chrysogenum* fermentation processes.[24,28] Accurate estimation of μ was made possible by this data reconciliation (DR) strategy. However, the reliable performance of DR based μ controller was limited by (i) generation of unforeseen metabolites, (ii) quality of measured signal, (iii) complex production medium.[24] Right choice of PAT tools for reliable μ estimation followed by an application of simple μ controller for broader range of bioprocess systems remains a quest for bioprocess engineers.[11,29]

In this present study, we developed a reliable μ estimator based on real-time capacitance measurements and successfully controlled the methanol feed rate through developed modified PID (proportional, integral and derivative) control strategy for production of huIFNα2b in glycoengineered *Pichia pastoris*. PID is the most common and widely adopted control algorithm employed in various industries and has been universally accepted for the majority of engineering applications. Its robust performance at various operating conditions combined with its functional simplicity, allows easy and effective handling by process engineers as compared to advanced control techniques where it requires complicated mathematical approach and more computation to control the process.[30] Control of specific growth rates in the bioprocesses like bacterial, eukaryotic and mammalian cell systems were exclusively carried out for decades using PID control strategy.[21,31,32] Optimal PID output is associated with the reduction in noise obtained by varying its basic parametric coefficients of proportional, integral and derivative. This present investigation focusses on elucidating the role of μ on huIFNα2b production on huIFNα2b titer, specific huIFNα2b productivity and methanol accumulation based on insights gained from the real-time capacitance measurements. This first-of-its-kind study delineates the application of a simple robust real-time capacitance-based feedback algorithm to control μ especially at low range ($0.015 - 0.06\ h^{-1}$) during the induction phase.

MATERIALS AND METHODS

Strain and media

Recombinant *Pichia pastoris* SuperMan5 strain (Mut^+phenotype) expressing huIFNα2b was used in this study. The huIFNα2b expression is under the control of the AOX1 promoter and is secreted in the extracellular media with the help of α-factor signal. The construction of this strain has been described in our previous studies.[5,6] The stock culture was maintained at −80 °C, in yeast peptone dextrose (YPD) media containing 20% (*v*/*v*) glycerol. The media compositions used in this study are as follows:

- Starter culture medium (YPD): yeast extract 10 g L^{-1}; peptone 20 g L^{-1}; dextrose 20 g L^{-1}.
- Pre-culture medium (yeast extract peptone glycerol, YPG): yeast extract 10 g L^{-1}; peptone 20 g L^{-1}; glycerol 20 g L^{-1}.
- Optimized basal salt medium:[33] glycerol 48.84 g L^{-1}; K_2SO_4 18.2 g L^{-1}; $MgSO_4$ 7.28 g L^{-1}; KOH 4.13 g L^{-1}; $CaSO_4 \cdot 2H_2O$ 0.93 g L^{-1}; $(NH_4)_2SO_4$ 8.42 g L^{-1}; 85% H_3PO_4 26.7 mL L^{-1}; PTM4 salts 4.4 mL L^{-1}. The composition of PTM4 salt solution: 2 g L^{-1} $CuSO_4 \cdot 5H_2O$, 0.08 g L^{-1} NaI, 3 g L^{-1} g L^{-1} $MnSO_4 \cdot H_2O$, 0.2 g L^{-1} $Na_2MoO_4 \cdot 2H_2O$, 0.02 g L^{-1} H_3BO_3, 0.5 g L^{-1} $CaSO_4 \cdot 2H_2O$, 0.5 g L^{-1} $CoCl_2$, 7 g L^{-1} $ZnCl_2$, 22 g L^{-1} $FeSO_4 \cdot 7H_2O$, 0.2 g L^{-1} biotin and 1 mL L^{-1} H_2SO_4 98% (*v*/*v*).
- Methanol feed solution: methanol 100% (*v*/*v*) + 12 mL PTM4 salts per 1 L of methanol.

Inoculum preparation

The starter culture was prepared by inoculating 5 mL of YPD medium with recombinant *Pichia pastoris* (SuperMan5 expressing

 © 2019 Society of Chemical Industry

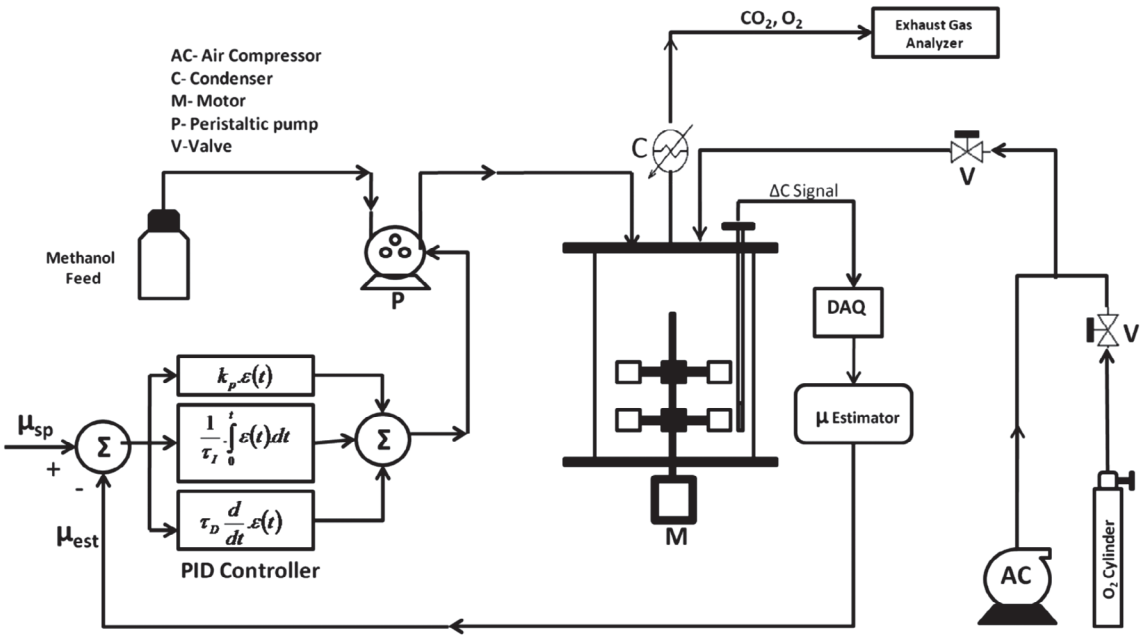

Figure 1. Schematic representation of bioreactor experimental setup with the PID control of specific growth rate based on capacitance signal.

huIFNα2b) from the glycerol stock vial stored at −80 °C. Pre-culture was prepared by inoculating starter culture in 1-L baffled Erlenmeyer flask containing 170 mL of sterile YPG medium. The inoculum was incubated at 30 °C and 220 rpm for 24 h to a final OD_{600} of 2 to 4.

Bioreactor operation

Pichia pastoris huIFNα2b fermentation was carried out in a 2.7 L bioreactor (Biojenik Engineering, Chennai, India), which was equipped with a bottom driven 6 blade Rushton turbine to achieve an efficient oxygen transfer rate (OTR). Basal salt medium autoclaved at 121 °C under 1 atm pressure was transferred aseptically into the reactor. Fermentation was initiated by the addition of preculture (10% *v/v*) and working volume (V_R) was maintained at 1.7 L. The real-time process signals, namely capacitance (in pF cm^{-1}), conductivity (in mS cm^{-1}), dissolved oxygen (%), temperature (°C), pH, methanol feed (in grams) and methanol feed rate (in mL h^{-1}) were acquired by NI 6238 Data Acquisition (DAQ) hardware (National Instruments, Austin, TX, USA) with a maximum sampling rate of 250 kS s^{-1} per channel. The acquisition of agitation rate was governed by a parallel DAQ device (NI 6002, National Instruments) operating in tandem with the NI 6238 hardware. A supervisory control and data acquisition (SCADA) interface was developed indigenously using a graphical programming interface (LabVIEW, National Instruments) platform, which governs data logging (every 5 s interval), data preprocessing (e.g. moving average, noise filtering), data display (graphs, archiving) and control algorithms as indicated in Fig. 1. Reaction (growth) temperature was maintained at 30 °C and pH was maintained at 5.4 by the addition of 25% (*v/v*) ammonia solution, and 30% (*v/v*) phosphoric acid (H_3PO_4), as neutralizing agents. Batch mode reactor operation was set to continue until complete utilization of glycerol, which was indicated by a sharp rise in dissolved oxygen (DO) signal.

Offline analysis

Optical density measurements of the collected samples were performed at 600 nm (OD_{600}) using an UV-visible spectrophotometer (GE Healthcare, Hatfield, UK). Biomass concentration (in g L^{-1}) was estimated by transferring 1 mL of the fermentation broth into pre-weighed 1.5 mL tubes and centrifuging them at 13000 rpm for 10 min at 4 °C. The supernatant was separated, and stored at −20 °C for offline analysis of glycerol and methanol through high-performance liquid chromatography (HPLC) and huIFNα2b concentration estimation by enzyme-linked immunosorbent assay (ELISA) analysis was as described earlier.[33]

Estimation of specific growth rate (μ_{est})

Dielectric spectroscopic investigation involves capacitance and conductivity measurements of reaction broth containing biomass, product and other analytes.[34] Capacitance probe (Aber Instruments, Aberystwyth, UK) is segregated into an apex ceramic portion containing two annular electrodes and a tapering part extended sufficiently to be immersed into the reaction broth. Head amplifier connected to the probe generates an electric field across the annular electrodes by an applied frequency (0.1–20 MHz). Futura tool (Aber Instruments), an in-built application, records the capacitance, *C* (0–200 pF cm^{-1}), and conductivity, *G* (0–40 mS cm^{-1}), at dual frequencies (580 kHz and 15.560 MHz). The ΔC and ΔG values were obtained by subtracting response signal at measurement frequency (580 kHz) from the signal at the reference frequency (15.560 MHz). Sampling rate of the capacitance signal was further amplified (10 000 samples s^{-1}) by connecting the probe transmitter to the NI 6238 DAQ device. Mean averaging of ΔC and ΔG at every 100 data points was dealt in order to reduce the noise associated with signal acquisition.[35] Specific growth rate was estimated by using real-time capacitance measurements on a moving window frame of 2 h interval and was computed by Eqn (1). The interval of 2 h was maintained, considering the slow growth dynamics of *Pichia pastoris* (SuperMan5) strain during methanol induction phase (doubling time ≈ 12 h) and ensuring reliable prediction of estimated specific growth rate (μ_{est}). Thus real-time values of μ_{est} serves to process inputs in the proposed PID control and were logged at 5 s intervals.

$$\mu_{est} = \frac{\ln(\Delta C_{t,n}) - \ln(\Delta C_{t,n-1})}{(t_n - t_{n-1})} \quad (1)$$

 © 2019 Society of Chemical Industry

Investigation on the effect of the feeding strategies on μ_{est}

During the fed-batch phase, two distinct feeding strategies, namely pulsed feeding and exponential feeding regulated by PID feedback loop were deployed to study the effect on μ_{est}. The former one deals with addition of defined amount of methanol (first pulse) after complete consumption of glycerol, allowing methanol to be utilized fully and replenished again (second pulse). This procedure was repeated at regular time intervals to ensure the C-source was available at regular intervals during induced phase growth. The feedback control strategy adopted in this study compares the parsed μ_{est} values to its set point, μ_{sp}. PID controller manipulates the output and adjusts the feed rate in order to minimize error between process input and set value (Fig. S1, Supporting Information). Reliability of μ_{est} model was validated by offline OD_{600} measurements.

Feed rate control

Pulsed feed rate

The complete consumption of residual glycerol in the batch culture was indicated by a rapid rise in DO signal accompanied by a sudden drop in both carbon dioxide emission rate (CER) and oxygen uptake rate (OUR) signals. The first methanol pulse (20 g) was initialized to achieve a final concentration of 1.48% *v/v* (11.8 g L^{-1}) of pure methanol (supplemented with 12 mL of PTM4 per 1 L of methanol), in the reaction broth. Preliminary experiments suggested that 1.48% (*v/v*) as optimum methanol concentration for increased huIFNα2b production and hence, repeated methanol pulses with a final concentration of 1.48% (*v/v*) was continued to assess the effect of optimal methanol pulse on cell metabolism (growth and protein production). The influence of excess methanol on cell metabolism was also investigated by addition of first methanol pulse (30 g) to attain the final concentration of 2.2% (*v/v*) with pure methanol (supplemented with 12 mL of PTM4 per 1 L of methanol) followed by repeated pulsed methanol addition (final concentration of 2.2% *v/v*). Complete utilization of methanol was indicated by a rapid rise in DO signal and a drop in OUR/CER signals. Samples were collected at regular time intervals for the assessment of DCW (Dry Cell Weight), huIFNα2b titer and residual methanol concentrations and the resultant average values plotted against time.

Exponential feed rate

The control of μ at its desired set point value is achieved by feeding the limiting substrate in proportion to the exponential rate of increase in cell concentration. The rate of exponential feeding typically establishes quasi-steady between substrate affinity (k_S) and residual substrate concentration (S) in the reaction broth, which significantly influences the μ value. This feeding strategy is advantageous for any Monod's type of microbial growth and attempts to maintain the methanol concentration (limiting substrate) well above its k_S value. The feed rate equation as shown in Eqn (2) contains feed-forward and feedback controller components. The former initializes a consistent feeding of limiting substrate (methanol) with respect to the initial biomass concentration, which was developed till batch growth phase, i.e. glycerol phase and the latter component determined the positive/negative exponent of the feed rate control.[27] The feed rate is governed by,

$$F_{FB} = F_0 e^{(\mathrm{PIDO}/P).t} \tag{2}$$

Where F_{FB} is methanol feed rate regulated by feedback controller (in mL h^{-1}) and F_0 is feed forward component (in mL h^{-1}).

The performance of classical controllers in bioprocess systems is challenged by several factors, which includes dynamic process conditions, cell metabolic perturbations and instability due to exponential increase in process disturbances.[36–38] A slight modification is adopted in the controller algorithm by including the proportional, integral and derivative terms directly into the exponent term of the growth equation (Eqn (4)), which could enhance the controller robustness.[24] PID controller computes error based on Eqn (3) and actuates the positive/negative exponent function in response to real-time μ values. PID control loop was designed (Fig. S1) such that exponential feeding rate during methanol phase was regulated by PID output (PID O/P) and represented by Eqn (4). The main motivation of this approach is that the inherent simplicity of the formulation should contribute to greater controller robustness.

$$\varepsilon(t) = \mu_{sp}(t) - \mu_{est}(t) \tag{3}$$

$$\mathrm{PIDO}/P = k_p.\varepsilon(t) + \frac{1}{\tau_I}.\int_0^t \varepsilon(t).dt + \tau_D.\frac{d}{dt}.\varepsilon(t) \tag{4}$$

The selection of controller parameters, namely proportional controller gain (k_p), integral time (τ_I, in minutes) and derivative time (τ_D, in minutes) plays a pivotal role in the PID controller performance due to the exponential increasing trend of μ related disturbances. The manual tuning method was employed systematically in this study for appropriate selection of the controller parameters.[39] Feed-forward component, F_0 was determined by estimating initial biomass concentration during glycerol phase (X_0) and substituted in the following relationship[40] (Eqn (5))

$$F_0 = \frac{X_0 V_0 \mu_{sp}}{S_{met} Y_{X/met}} \tag{5}$$

where V_0 reactor volume is at the end of glycerol phase, S_{met} is methanol concentration in feed stream (793 g L^{-1}), and $Y_{X/met}$ is biomass yield during methanol phase.

Methanol feed during induction phase was carried out by a high precision variable speed pump (Watson Marlow 120 U, Falmouth, UK) and was connected to the PID loop. Feed rates were already pre-calibrated with a current of 4 to 20 mA, which operates the precision pump. PID O/P connected to the precision pump via 4–20 mA signal responses tightly control the dynamic feeding rate. The controller performance was evaluated by calculating the average absolute tracking error for each μ_{sp}. All the experiments were performed in duplicates and the average values are represented in the tables and figures.

Oxygen uptake rate (OUR) measurement

A laboratory scale exhaust gas analyzer (Ultramat 23, Siemens AG, Berlin, Germany) was used as a complimentary PAT tool to measure O_2 and CO_2 concentration in the off-gas (exit stream of bioreactor). The O_2 and CO_2 concentrations were measured by paramagnetic detection and IR based absorption techniques, respectively. Gaseous phase mole fractions of O_2 and CO_2 obtained from exhaust gas analyzer measurements was used to estimate OUR, r_{O_2} and CER, r_{CO_2} based on Eqns ((6) and ((7), respectively.

$$\mathrm{OUR} = \frac{\dot{m}_g}{V_R}\left[y_{O2,in} - y_{O2,out}\left(\frac{y_{inert,in}}{y_{inert,out}}\right)\right] \tag{6}$$

$$\mathrm{CER} = \frac{\dot{m}_g}{V_R}\left[y_{CO2,out}\left(\frac{y_{inert,in}}{y_{inert,out}}\right) - y_{CO2,in}\right] \tag{7}$$

 © 2019 Society of Chemical Industry

where m_g is mass flow rate of gas in L s^{-1}, V_R is the volume of the reaction broth in litres, $y_{O2,in}$ is mole fraction of O_2 in air inlet stream, $y_{O2,out}$ is mole fraction of O_2 in air outlet stream, $y_{CO2,in}$ is mole fraction of CO_2 in air inlet stream, $y_{CO2,out}$ is mole fraction of CO_2 in air outlet stream, $y_{inert,in}$ is mole fraction of N_2 in air inlet stream and $y_{inert,out}$ is mole fraction of N_2 in air outlet stream.

Volumetric rates, r_{O_2} and r_{CO_2} could provide direct insight on the cell physiology and their ratio indicates the respiratory quotient[41] of *Pichia pastoris*. OUR and CER values were estimated by SCADA and logged at every 10 s interval. The O_2 and CO_2 %(mole basis) of inlet air (ambient air) was regularly monitored by the exhaust gas analyzer in all the reactor runs and their average values maintained a high level of consistency within the range 20.85–20.9% and 0.02–0.04%, respectively.

Purification of recombinant huIFNα2b

Glycosylated huIFNα2b from the culture supernatant taken from the optimal control run ($\mu_{sp} = 0.04\ h^{-1}$) was purified as per the protocol described in our previous studies.[5,6] In brief the purification protocol included His-tagged affinity chromatography and Concanavalin A (Con A) chromatography steps sequentially. The pooled fractions containing major amounts of the recombinant huIFNα2b after His-tag affinity chromatography were subjected to Con A chromatography for the selective purification of glycosylated huIFNα2b.

Biological activity of recombinant huIFNα2b

Biological activity of the recombinant huIFNα2b was assessed by its ability to inhibit cell growth in the *in vitro* study using breast cancer cell lines (T47D and MCF7). T47D cell line and MCF7 cell line were maintained in RPMI medium and Dulbecco's modified Eagle medium (DMEM), a high glucose medium, respectively; both media were supplemented with streptomycin and penicillin antibiotic along with 10% fetal bovine serum (FBS). Cells were grown to 70% of confluence in humidified incubator at 37 °C and 5% CO_2. Thereafter, the adhered cells were washed with Dulbecco's phosphate buffered saline (DPBS) and detached using 0.25% trypsin-ethylenediaminetetraaceticacid (EDTA). About 1×10^4 cells $well^{-1}$ were transferred into a 96-well cell culture plate and incubated overnight at 37 °C and 5% CO_2 for further study. The spent medium was replaced by 200 µL of fresh medium containing either commercial IFN α2b drug or purified recombinant huIFNα2b at different concentrations, 0.5, 7.5, and 20 nM. Cells in the medium without IFN α2b were used as a negative control. The antiproliferative activity of the huIFNα2b was determined after 96 h of treatment. The viable cell densities were detected after washing with DPBS based on the conversion of MTT into formazan by mitochondrial reductase. 100 µL of MTT (0.5 mg mL^{-1}) was added to each well and incubated at 37 °C for 3 h. The MTT solution was discarded and the insoluble formazan crystals were dissolved in 100 µL dimethyl sulphoxide (DMSO) and incubated at 25 °C for 5 min. The absorbance was measured at 570 nm with the reference absorbance of 690 nm. The assay was performed in five replicates.

RESULTS AND DISCUSSION

Specific growth rate estimator (μ_{est})

Pichia pastoris huIFNα2b fermentation runs exhibited a linear correlation ($R^2 > 0.9$) between capacitance and biomass concentration (DCW) data (Fig. S2, Supporting Information). Segregation of various phases such as growth, transition and induction phases could be observed from ΔC signal profile (Fig. S3, Supporting Information). The proportional rise in ΔC signal with respect to an increase in biomass concentrations signal were found to be consistent ($R^2 = 0.988$ and $R^2 = 0.911$ for two different batch experiments) during all the stages of cultivation, namely exponential, methanol induction, methanol-limited and starvation phases of growth. The rate of change in the capacitance value with respect to time was modelled to provide real-time estimation of specific growth rate (μ_{est}). Reliability of the estimated values (μ_{est}) was validated by comparison with $\mu_{offline}$ data estimated using DCW measurements in accordance with the published reports.[24] The proposed μ_{est} estimator (Eqn ((1)) deciphered from ΔC signal, was thus deployed to read calculated μ values at different regimes of *Pichia pastoris* growth. The relationship between the increments in capacitance value to the DCW during the induction (production) phase was estimated to be an average of correlation obtained from different fermentation runs (Biomass = (6.209)ΔC) (Fig. S2). The average slope value for biomass and ΔC correltation for induction phase (6.209) was observed to be significantly greater than the exponential growth phase (3.693). This could be attributed due to the fact that 'glycerol' is preferred as 'anabolic' substrate and 'methanol' serves as 'energetic' substrate driving the protein production in *Pichia pastoris* fermentation.[25,42]

Growth characteristics of *Pichia pastoris* during growth and induction phases of huIFNα2b production

Growth phase is characterized by the utilization of glycerol, which shows repressing effect on the AOX transcription elements. As a result it leads to the channelling of major carbon flux towards biomass formation with relatively lesser maintenance requirement.[43] This can be observed from the higher biomass yields ($Y_{X/gly}$) achieved at the end of glycerol batch phase as shown in Table 1. During the batch growth phases of pulsed feed strategy (glycerol as sole carbon source), significant biomass production was achieved (Table 1). Sudden drop in the respirometric activity (decrease in CER and OUR signal) and a drastic rise in DO signal indicated the exhaustion of glycerol in the reaction broth. Their levels therefore acted as alarms that signalled the completion of batch glycerol growth phase (Fig. S3). After the complete utilization of glycerol in batch growth phase, methanol (100% *v/v* methanol supplemented with PTM4 salts) adaptation pulse was added as a supplement, which marked the initiation of transition phase. The latter was characterized by the decrease in viable cell volume post methanol addition, subsequently manifested by the drop of ΔC signal (Fig. S3). Methanol pulses (four shorter pulses of 5 g of methanol) were continued until the response from ΔC signal showed a positive upfront. This phase is also regarded as the adaptation phase, in which AOX transcription machinery gets gradually activated and carbon assimilation is shifted from glycerol to methanol after about a duration of 3 to 4 h. Induction phase starts at the pulsed feeding of methanol by the methodology as described in the 'Pulse Feed rate' section previously, after the transition phase. Different dosage rates of methanol used, i.e. optimal (20 g) and excess (30 g), its influence in biomass yield and huIFNα2b titer are reported in Table 1. Pulsed feeding rate at different levels was found to have negligible effect on their respective μ_{est} values as observed in Table 1. Specific rate of methanol utilization ($q_{s,met}$) was determined for two different methanol pulsed feeds (20 and 30 g) and the residual methanol concentration plot (Fig. 2(A)) showed that the methanol was fully utilized in both

 © 2019 Society of Chemical Industry

Table 1. Assessment of pulsed feed strategy on estimation of specific growth rate (μ_{est}) during methanol induction phase

Pulsed feed rate	DCW (g L^{-1})	μ_{gly} (h^{-1})	μ_{met} (h^{-1})	$Y_{X/gly}$ (g g^{-1})	huIFNα2b (mg L^{-1})	Volumetric productivity,[a] r_p (mg L^{-1} h^{-1})	$Y_{X/met}$ (g g^{-1})
Batch run with pulse feeding (20 g methanol)	158.4	0.213	0.02718	0.772	436	6.22	0.129
Batch run with pulse feeding (30 g methanol)	133.12	0.204	0.0262	0.822	627	10.11	0.109

[a] r_p was computed during induction phases only.

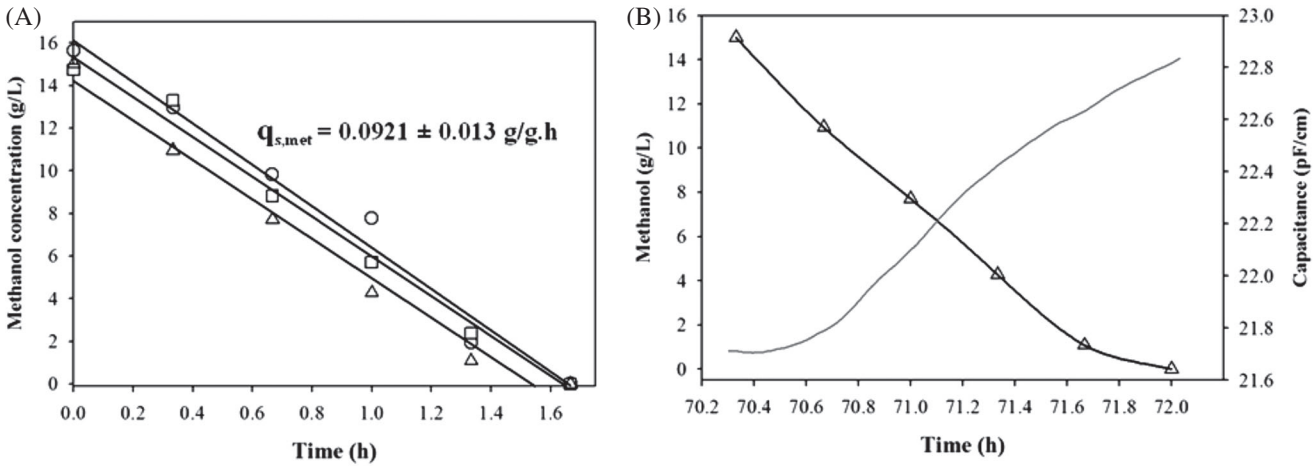

Figure 2. (A) Dynamic methanol uptake profile by *Pichia pastoris* cultivation during repeated methanol pulse feeding at the induction phase: duration 62–64 h (open circles), duration 70–72 h (open triangles), duration 77–79 h (open squares). $q_{s,met}$ was calculated from the ratio of volumetric methanol utilization (g L^{-1} h) to biomass concentration. (B) Influence of methanol (open triangles) utilization (g L^{-1}) on developed capacitance signal (ΔC) (pF cm^{-1}) (continuous dark grey line) at 70–72 h.

the feed conditions. $q_{s,met}$ estimated for the different pulsed feed (20 g and 30 g) rates were found to be consistent at an average of 0.0921 ± 0.013 g g^{-1} h^{-1} throughout the induction phase (Fig. 2(A)) while the ΔC signal was positively influenced by the concomitant methanol utilization by the *Pichia pastoris* (Fig. 2(B)).The specific methanol utilization rate ($q_{s,met}$= 0.0921 ± 0.013 g g^{-1} h^{-1}) in this heterologous expression system was several folds higher than that reported for any of the de-repressed substrates[44] and also was found to be constant throughout the production phase (Fig. 2(A)). During the time course of methanol utilization in the pulse feeding strategy, the μ_{met} of *Pichia pastoris* varies dynamically showing maximum μ_{met} at higher methanol concentrations, i.e. immediately after supplementing 20/30 g feed bolus and as the methanol depletes, μ_{met} drops proportionally towards zero.[45] Increase in μ_{met} at the sudden onset of feed could be traced from an increase in ΔC signal (Fig. 2(B)). Thus it indicates that the cell metabolism is limited by the methanol feed, leading to its effective assimilation and followed by a flattened profile representing methanol depletion. Therefore, it proves the fidelity of the ΔC signal to indicate/signal the physiological state of the *Pichia pastoris* during induction phases. Also, the dynamic profiles of methanol concentration (Fig. S4, Supporting Information) indicated that the kinetics of biomass growth is independent of the dosage rates. The huIFNα2b titer (627 mg L^{-1}) was significantly higher for excess pulse feeding (30 g) as shown in Table 1, in spite of μ_{met} value remaining almost unchanged. These findings suggest that pulsed addition of methanol at its temporal excess (30 g) influenced the huIFNα2b production positively at the expense of reduction in biomass yield ($Y_{X/met}$). The possibility of inhibitory effects of methanol on membrane synthesis and DNA replication lead to decrease in the biomass growth and resulted in regulation of energy flux (as a result of methanol utilization) towards huIFNα2b synthesis pathway, which in turn lead to enhancement in the product titer.[46] The constructed recombinant glycoengineered *Pichia pastoris* in this study exhibits a better stability in expressing AOX transcription genes amidst higher methanol concentrations in the range 14–16 g L^{-1} as shown in Fig. 2(A, B). This is substantiated by reports suggesting that recombinants with the integration of gene of interest possessed higher methanol tolerance compared with wild type strain[46,47]

Design of PID feedback loop for the exponential methanol feeding strategy at different μ_{sp}

In all μ_{met} control runs, the batch growth phase lasted for a duration of up to 26–28 h leading to complete glycerol consumption and generated 35–40 g L^{-1} of biomass. Larger proportion of glycerol consumption, i.e. more than 80% of substrate ($Y_{X/gly}$> 0.8 in Table 2) was used for/directed towards the synthesis of biomass, thus generating the required potential cell machinery (high cell density) for the subsequent huIFNα2b production. Adaptation phase encompassed four to five shorter methanol pulses required to activate de-repressed methanol induced AOX transcription genes. In induction phase, exponential feeding strategy was designed such that methanol accumulation was maintained less than its critical level (>15 g L^{-1}) based on the published resources.[48] Continuously regulated feed was initiated following the adaptation phase in all control runs intended to maintain a different specific growth rate at the desired set point values

 © 2019 Society of Chemical Industry

Table 2. Assessment of feedback control strategies employing different set point specific growth rate (μ_{sp})

μ_{sp} (h^{-1})	DCW ($g\ L^{-1}$)	r_x ($g\ L^{-1}\ h^{-1}$)	μ_{gly} (h^{-1}) (offline)[a]	μ_{met} (h^{-1}) (offline)	$Y_{X/gly}$ ($g\ g^{-1}$)	huIFNα2b ($mg\ L^{-1}$)	Volumetric productivity,[b] r_p ($mg\ L^{-1}\ h^{-1}$)	$Y_{X/met}$ ($g\ g^{-1}$)
0.015	119.8	1.61	0.233	0.0181	0.853	550.3	13.75	0.154
0.03	135.76	2.088	0.229	0.0378	0.817	980.4	25.8	0.157
0.04	185.52	2.829	0.252	0.0464	0.88	1483.7	39.04	0.262
0.06	124	2.005	0.245	0.063	0.858	536.2	15.77	0.176

[a] Maximum specific growth rate estimated during growth phase.
[b] r_p was computed during induction phases only.

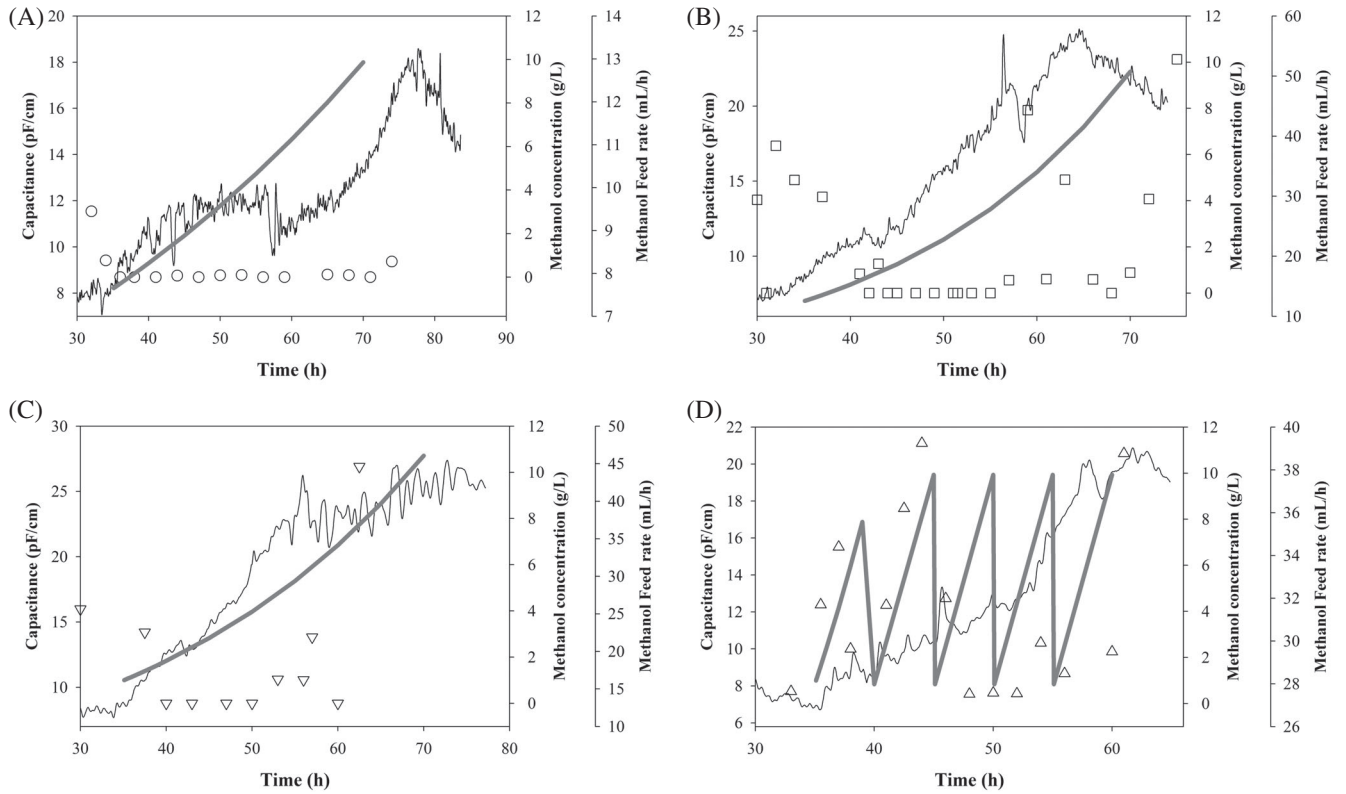

Figure 3. Exponential feedback control of methanol (dark grey line) during induction phase: Capacitance signal, ΔC (dark continuous line); methanol (dark grey line); scatter plots representing methanol concentration values during various μ_{sp} runs: (A) open circles ($\mu_{sp} = 0.015\ h^{-1}$), (B) open squares ($\mu_{sp} = 0.03\ h^{-1}$), (C) down-facing open triangles ($\mu_{sp} = 0.04\ h^{-1}$), (D) up-facing open triangles ($\mu_{sp} = 0.06\ h^{-1}$).

($\mu_{sp} = 0.015$, 0.03, 0.04 and 0.06 h^{-1}). The feed-forward and feedback controller parameter (obtained from Eqn 2) were given as input in the SCADA before proceeding with the μ_{met} control. The lowest (7.65 mL h^{-1}) and highest initial feeding rate (28.15 mL h^{-1}) of methanol were decided based on desired μ_{sp}values of 0.015 and 0.06 h^{-1}, respectively in the feed-forward component of Eqn (5). The performance of the implemented feedback PID control strategy manipulating methanol feed rate to control μ_{met} in response to various μ_{sp} values were tabulated in Table 2. In all μ_{met} control runs except $\mu_{sp} = 0.06\ h^{-1}$, exponential feeding rates were observed to be effective (Fig. 3(A–C)) in meeting the biomass growth and protein production requirements owing to the complete utilization of methanol (residual methanol concentration was observed closer to zero for more than 20 h). Rapid consumption of methanol in all control runs substantiates that dynamic mass balance was established by the PID controller between methanol availability (feed stream) and its immediate consumption by *Pichia pastoris*. The ΔC signal was observed to be a good indicator of methanol assimilation, as it rises sharply during the early induction phase representing effective methanol utilization. In a similar manner, methanol accumulation (Fig. 3(A–C)) in the later induction phase results in the stabilization of ΔC signal after 60 h. OUR/CER signals corroborated well with ΔC signal in distinct phases of *Pichia pastoris* huIFNα2b production, but associated with perturbations and noises due to the regulation of airflow rate in order to maintain the desired DO concentration (Fig. S3). Respiratory quotient (RQ) of 0.683 ± 0.128 determined from different μ_{met} control runs illustrated the metabolic utilization efficiency of carbon source (glycerol/methanol) and this value corroborated with other *Pichia pastoris* variants reported.[49,50] Exponential feeding of methanol resulted in effective utilization of methanol for biomass formation ($Y_{X/met}$ =0.262 $g_{biomass}\ g_{methanol}^{-1}$)

 © 2019 Society of Chemical Industry

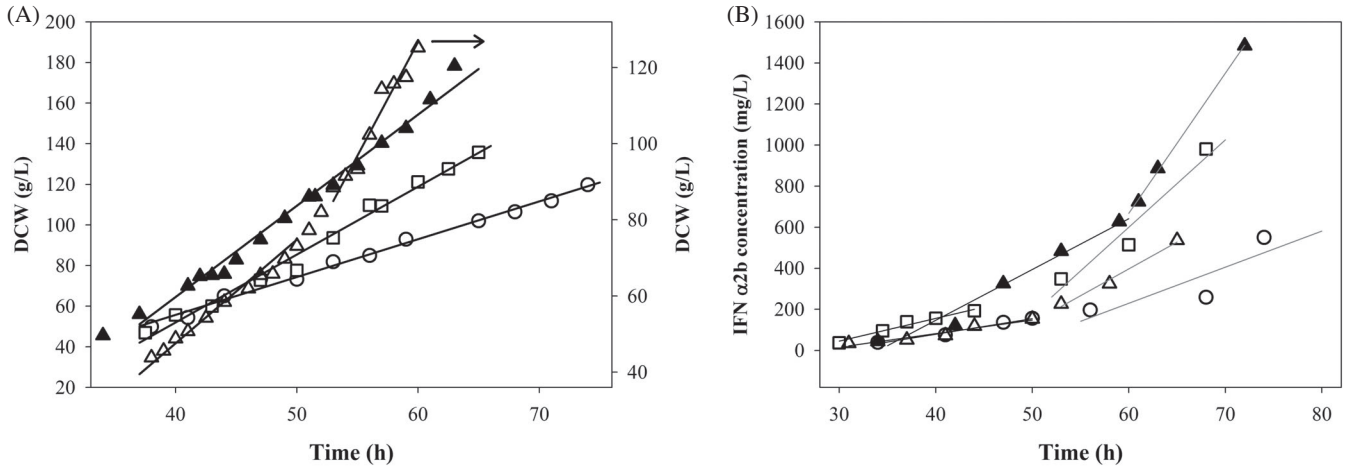

Figure 4. (A) Influence of specific growth rate on DCW and (B) influence of specific growth rate on huIFNα2b production: open circles ($\mu_{sp} = 0.015\ h^{-1}$), open squares ($\mu_{sp} = 0.03\ h^{-1}$), filled triangles ($\mu_{sp} = 0.04\ h^{-1}$), open triangles ($\mu_{sp} = 0.06\ h^{-1}$)

for $\mu_{sp} = 0.04\ h^{-1}$. At higher μ_{sp} (0.06 h^{-1}), the exponential feed rate was repeated at regular time intervals rather than proceeding at a continuous feeding to avoid methanol accumulation to its critical level. By re-initializing the controller (Fig. 3(D)) at regular time intervals, the methanol feed rate was maintained between the range 27.98 and 37.77 mL h^{-1} in order to maintain the methanol concentration below its critical level. In spite of this repetitive feed strategy, significant methanol accumulation (4–10 g L^{-1}) was observed at the early induction phase (35–45 h) for the control run at $\mu_{sp} = 0.06\ h^{-1}$ (Fig. 3(D)). Also, residual methanol concentration consistently exhibited increasing and decreasing trends at regular intervals (Fig. 3(D)). Repeated exponential feed rate showed a passive response for biomass growth during early phases of induction, but later the cells adapted to high methanol load conditions exhibiting the controlled μ_{met} (substantiated by both μ_{est} and $\mu_{offline}$ values). Feed rate exceeding beyond maximum substrate uptake capacity (q_S^{max}) of *Pichia pastoris* led to the methanol accumulation especially for $\mu_{sp} = 0.06\ h^{-1}$ run. The glycoengineered *Pichia pastoris* (Superman 5) exhibits μ_{max} at 0.0624 h^{-1}, which leads to an excessive metabolic load on allocating carbon towards various activities. The imbalance between methanol feeding and subsequent utilization towards growth and protein production (Fig. 3(D)) is manifested by the metabolic perturbations experienced by organism, while almost attaining its maximum growth rate conditions.[51] The decrease in biomass growth (Fig. 4(A)) confirms the outcome of metabolic stress experienced by the *Pichia pastoris* growing at high specific growth rate ($\mu_{sp} = 0.06\ h^{-1}$). Inspite of the methanol accumulation, the controller maintained the μ_{est} at 0.0597 h^{-1} (near to μ_{sp}) at later phases of induction for 20 h.

Control characteristics of capacitance based μ_{est}

Dynamic variation of μ_{sp} to different set values in a single control experiment could be an attractive option from an operational perspective,[52] but would in turn exert dynamic pressure on AOX machinery of *Pichia pastoris*. This would lead to various levels of stress (transient adaptation of cells to different methanol concentrations) and complicate the interpretation of the protein expression level. Independent assessment of huIFNα2b production by controlling μ_{met} at different set point values would be advantageous, as the selective pressure applied on the AOX expression system by methanol feed is uniform throughout the induction phase. The proposed schema of the μ_{met} control as illustrated in Fig. S1 is highly dependent upon the PID tuning parameters and control characteristics.

In the entire controller tuning experiments, each tuning parameter was set and maintained for at least 8 h duration for observation. Controller gain (k_C), a ratio between methanol feeding rate (F_M) to the developed μ_{est} is a prominent factor[21] in establishing a stabilized controller output. The k_C value was maintained in the range between 0.5 and 1.0 and delivered robust controller performance for $\mu_{sp} \leq 0.04\ h^{-1}$. The 'integral' component of the controller was attributed to reduced offset in the controlled variable and to delivering a stable response. Ratio between methanol feeding rate (F_M) to μ_{est} is determined by the controller gain, k_C; it was set to ≤ 1, in order to avoid accumulation of methanol to toxic levels. Influence of tuning parameters over μ_{est} signal and their deviation with the proposed μ_{sp} are shown in Supporting Information Table S2. PID controller output was observed to be robust to meet the methanol demand for the biomass growth and huIFNα2b production owing to its effective consumption in the control experiments (Fig. 3(A, C)). Moreover, the methanol accumulation did not exceed the residual concentration (> 2 g L^{-1}) for biomass growth and remained consistent for long duration in all the control experiments except for μ_{sp} of 0.06 h^{-1} (Fig. 3(D)). At higher μ_{sp} say 0.06 h^{-1}, k_C was set to 4.8 to regulate the PID loop. The disproportion in the ratio between feeding rate and μ_{est} signal was key to the excessive supplementation of methanol over a shorter time frame. However, a discontinuous phase of controller regulation at $\mu_{sp} = 0.06\ h^{-1}$ attributed to the proposed $\mu_{offline}$ values.

Noise pretreated μ_{est} values obtained from ΔC signal at a time frame of every 2 h was compared with their corresponding offline values ($\mu_{offline}$) estimated from DCW measurements. The concurrence between μ_{est} and $\mu_{offline}$ values with respect to μ_{sp}, proves the successful accomplishment of the PID control (Fig. 5(A–D)). Lower average tracking error (less than 15%) obtained for all μ_{met} control runs showing that μ_{est} is in good synchronization with their respective set points (Table S3, Supporting Information). Moreover, the characteristics of controller especially the long-term stability could be effectively addressed in individual control experiments run at different μ_{sp} values. At different control μ_{sp} runs, a uniform control regime was maintained by feedback

 © 2019 Society of Chemical Industry

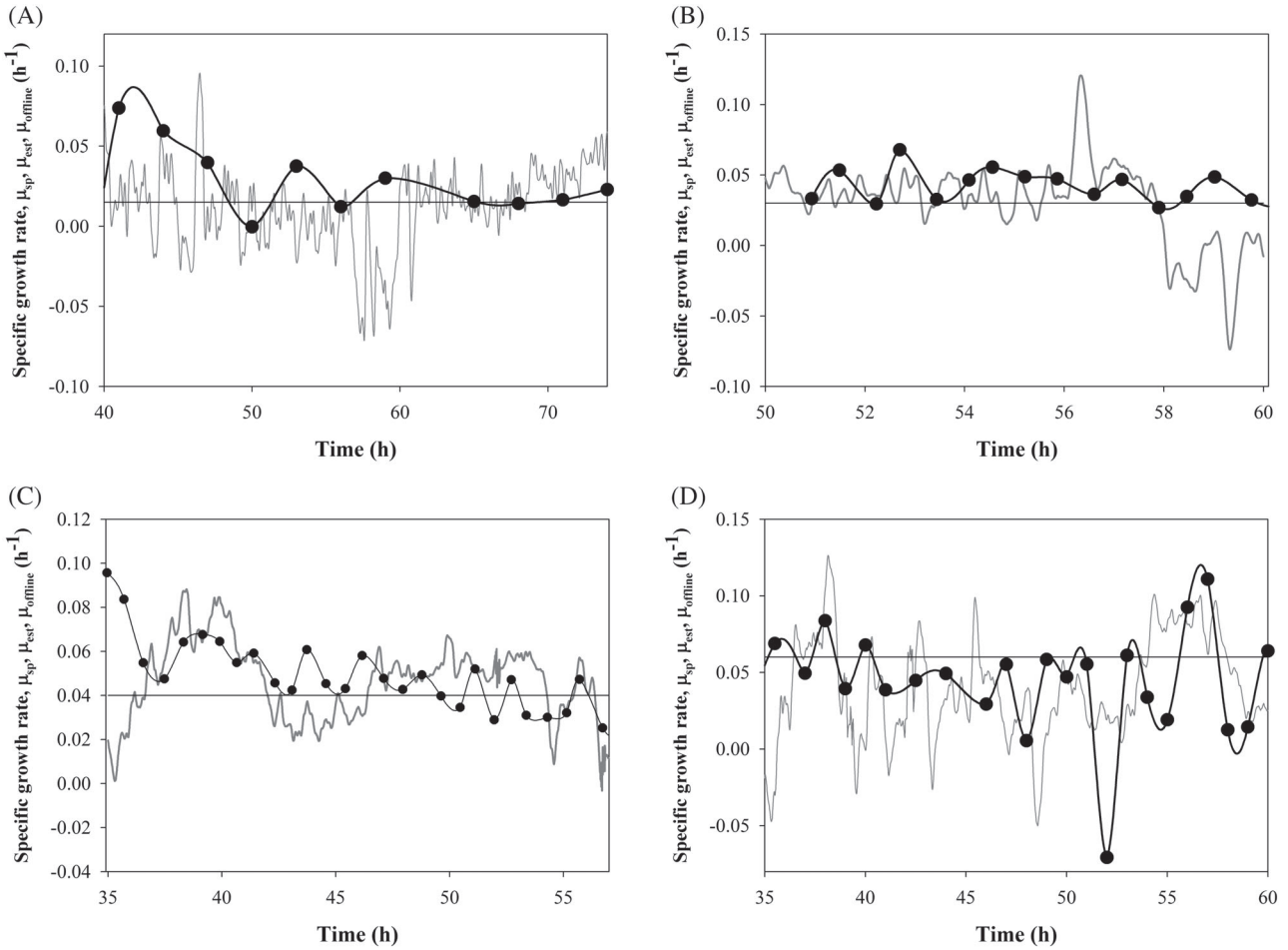

Figure 5. PID controller performance based on comparative evaluation of μ_{sp}, μ_{est} and $\mu_{offline}$ values: dark continuous lines represents μ_{sp}, dark grey continuous lines represents μ_{est}, filled circles with continuous line represents $\mu_{offline}$

control resulting in consistent biomass and huIFNα2b production (Fig. 4(A, B)). From Table 2, huIFNα2b production is strongly influenced by μ_{met} especially when maintained at a narrow range.[20,53] Thus, μ_{est} values were corroborated well with $\mu_{offline}$ measurements (Fig. 5). Exponential feeding of methanol regulated by PID loop proved to be more accurate/categorical/effective in maintaining a low μ_{sp} at a narrow range (0.015 – 0.06 h^{-1}) reported elsewhere.[21]

The oscillatory behaviour observed in μ_{est} in all the control runs (Fig. 5(A – D)) is attributed due to natural metabolic response of the *Pichia pastoris* but it is unlikely to become the controller effect and non-aligned to actual value of specific growth rate.[24] Similar oscillatory behaviour was observed during the exponential batch growth phase (glycerol), where *Pichia pastoris* was expected to grow at its maximum specific growth rate (μ_{max}). The error value for the optimal μ_{sp} (0.04 h^{-1}) run was found to be extremely low (0.0068 h^{-1}) and a consistent response (μ_{est}) for a long duration (> 10 h) was observed for different μ_{sp} values (Fig. 5(A – D)). The PID controller performance (long-term stability and tracking error) addressed in this study is observed to be better than the DR-based feedback control strategy reported.[24] During induction phase, *Pichia pastoris* experiences higher transcriptional load owing to lower huIFNα2b titer coupled with biomass growth and any attempt to cultivate the organism *Pichia pastoris* at higher μ_{met}, will result in μ_{est} oscillation with larger amplitude (evident from Fig. 5(D)).

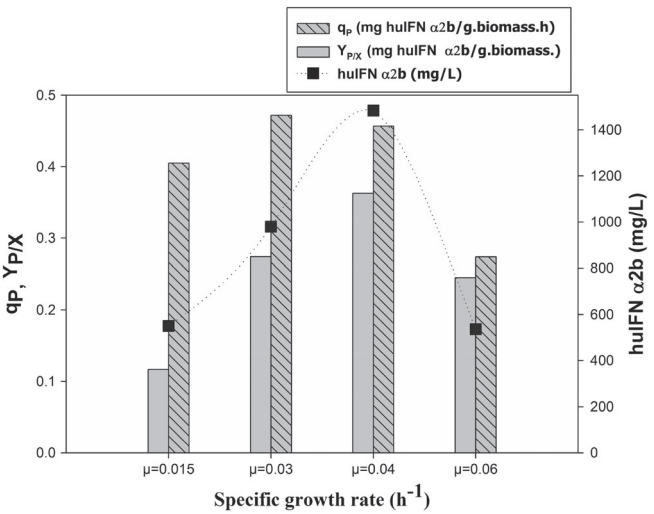

Figure 6. Influence of different specific growth rate (μ_{sp}) on huIFNα2b titer, specific productivity (q_P) and protein yield coefficient ($Y_{P/X}$).

Improvement in huIFNα2b productivity

The production of huIFNα2b was found to increase in conformity with DCW in every μ_{sp} run. However, a linear trend in DCW was observed in contrast to the exponential fashion of the

 © 2019 Society of Chemical Industry

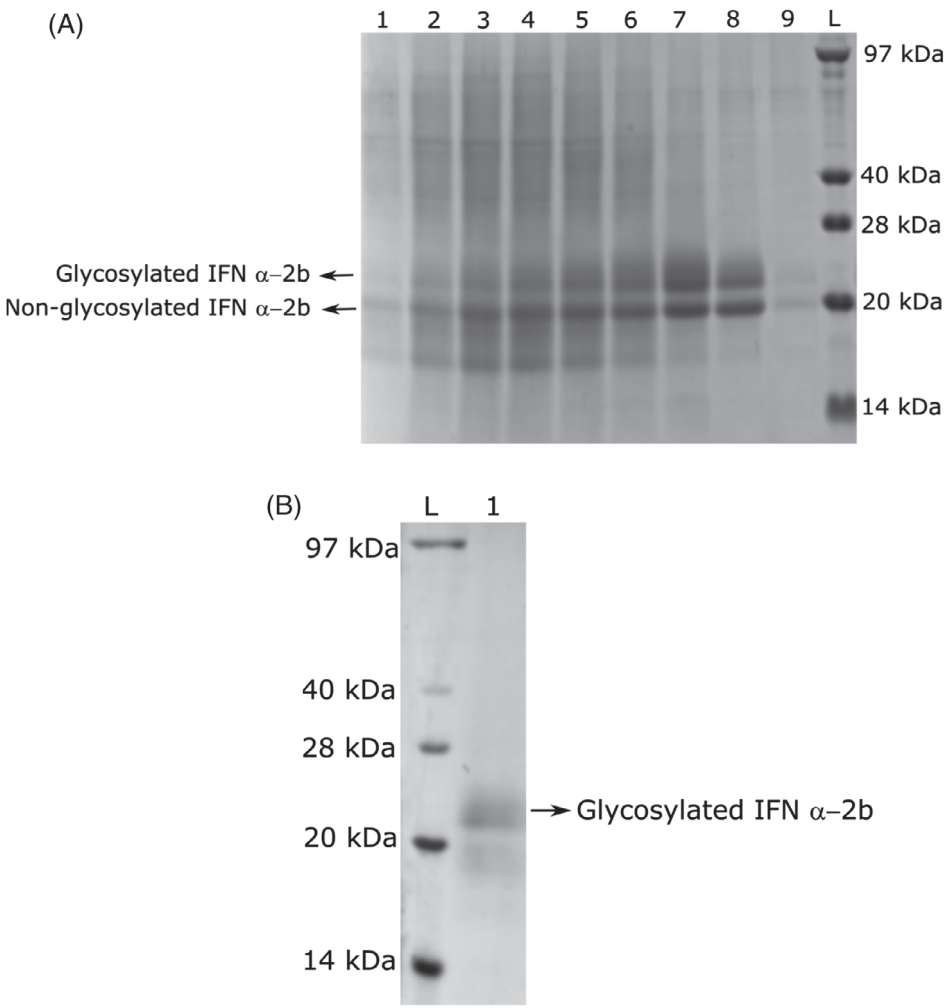

Figure 7. (A) Purification of recombinant huIFNα2b by His-tag affinity chromatography. Lanes 1–9 shows elution fractions and Lane L shows protein ladder. In Lanes 1–9, 25 µL of sample was loaded and in Lane L, 10 µL of protein ladder was loaded. (B) Purification of recombinant glycosylated huIFNα2b by Con A chromatography. Lane 1 shows elution fraction containing purified huIFNα2b and Lane L shows protein ladder. In Lane 1, 15 µL of sample was loaded and in Lane L, 10 µL of protein ladder was loaded.

huIFNα2b titers (Fig. 4(A, B)). The huIFNα2b production profile exhibited two distinct phases. During the first phase of induction (30–50 h), the specific protein productivities were at lower range, typically of 0.06–0.13 $g_{huIFN\alpha 2b}$ $g_{Biomass}^{-1}$ h^{-1}. At the second phase (> 60 h), the rate of increase in huIFNα2b titers quadrupled (0.26–0.47 $g_{huIFN\alpha 2b}$ $g_{Biomass}^{-1}$ h^{-1}) compared to their former phase in all μ_{sp} runs and a maximum of 1483 mg L^{-1} of product was achieved at $\mu_{sp} = 0.04\ h^{-1}$. Glycoengineered *Pichia pastoris* exhibited an elevated product titers ≥ 500 mg L^{-1} in all control runs and the volumetric productivity was found to be higher at $\mu_{sp} = 0.04\ h^{-1}$ (Table 2). The huIFNα2b titer, specific huIFNα2b production ($q_{huIFN\alpha 2b}$) and $Y_{P/X}$ were observed to increase with respect to exponential feeding of methanol till $\mu_{sp} \leq 0.04\ h^{-1}$, and decrease beyond this set point (Fig. 6). Repetitive feeding leading to methanol accumulation in $\mu_{sp} = 0.06\ h^{-1}$ run resulted in a moderate utilization of substrate when compared to other control runs. Moreover, the growth profile exhibited two different linear phases corresponding to 0.0271 h^{-1} and 0.0597 h^{-1}, respectively (Fig. 4(A)). The product titer (536 mg L^{-1}) obtained at the end of the fermentation was substantially reduced than other control runs.

From Fig. 6 it could be witnessed that both $q_{huIFN\alpha 2b}$ and $Y_{P/X}$ were found to be positively influenced by the increase in μ_{sp}. At different μ_{sp} based control runs with the corresponding methanol feeding rates in *Pichia pastoris* cultivation enabled the protein translation machinery to be exposed/subject to various levels of metabolic stress.[53] At higher specific growth rates, protein folding errors and heterogeneity was common in other recombinant proteins expressed in *Pichia pastoris*.[54] Methanol demand as a carbon and induction source competes for biomass growth as well as protein production. In case of *Pichia pastoris* cultivation at moderate growth rate (μ_{met}= 0.04 h^{-1}) conditions, the methanol concentration in the medium is expected to be utilized for central metabolism (growth and protein production) and a relatively higher carbon flux is diverted for protein (huIFNα2b) expression. Glycoengineered *Pichia pastoris* strain employed in this investigation is reported to have μ_{max} at 0.0624 h^{-1} during methanol induction phase. Relatively low protein titers resulted in the maximum μ_{sp} that could be addressed due to excessive AOX transcription burden. Specific huIFNα2b secretion rate, $q_{huIFN\alpha 2b}$ for $\mu_{sp} \leq 0.04\ h^{-1}$ was found to be greater than 0.4 mg g^{-1} h^{-1}, which emerges as the highest among different recombinant proteins expressed in glycoengineered *Pichia pastoris* under AOX promoter.[53,55,56] The huIFNα2b titer (1483 mg L^{-1}) obtained at $\mu_{sp} = 0.04\ h^{-1}$ is the highest reported value for *Pichia pastoris* and

 © 2019 Society of Chemical Industry

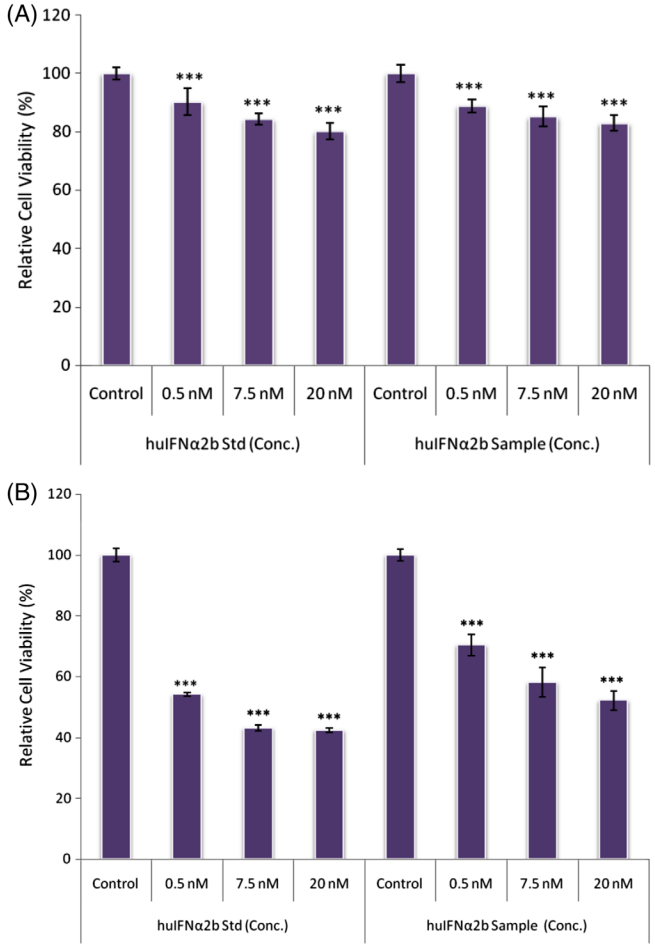

Figure 8. Antiproliferative effect of the purified huIFNα2b and standard huIFNα2b against breast cancer cell lines: (A) T47D and (B) MCF7. The assay was performed in five replicates. The values are statistically significant at ***$P < 0.001$ as analyzed by analysis of variance (ANOVA).

also for any other yeast expression platforms (Table S4 Supporting Information) reported in the literature.[57–62] Hence, this present study delineates that the specific growth rate is a paramount factor establishing superior specific protein productivity. Feedback control from a PID output is a relatively simpler methodology and robustly controlled the inducer feeding in response to the real-time signal (ΔC) than a pre-set feed-rate.

Purification and biological activity of recombinant huIFNα2b

The partial purification of the recombinant huIFNα2b (glycosylated and unglycosylated) from the mixture of other host cell proteins in the clarified supernatant was achieved by His-tag chromatography (Fig. 7(A)). The selective recovery of glycosylated huIFNα2b was achieved by Con A chromatography (Fig. 7(B)), where Con A binds to the terminal mannose of the glycan moiety attached to the glycosylated IFN α2b. The purification yield of recombinant IFN α2b was found to be 40% and was in good agreement with reported literature.[60]

Antiproliferative activity is one of the key biological attributes exhibited by huIFNα2b[63] and was assessed at varying concentrations of glycosylated IFN α2b using human breast cancer cell lines (T47D and MCF7). The biological activities of IFN α2b are driven by binding to the receptor complex (IFNAR1 and IFNAR2) and inducing JAK–STAT signalling pathway,[64] resulting in the activation of interferon-stimulated genes (ISGs). The growth inhibition by IFN α2b was more pronounced in the MCF7 (approximately 50%) cell line (Fig. 8(B)) compared to T47D (17%) cell line (Fig. 8(A)), and was also dose-dependent. This observation of higher huIFNα2b activity on MCF7 than the T47D cell line due to the higher expression levels of interferon receptors (IFNAR1 and IFNAR2) in MCF7 cell lines.[64] This effect of purified IFNα2b against T47D breast cancer cell line corroborated with the previously published reports[63–65] and also the human IFN α2b produced from *Escherichia coli* and *Pichia pastoris* X33 resulted in a 50% growth inhibition at a high concentration of 5 µg mL^{-1}.[63,65] It could be concluded that the observed antiproliferative effect is a result of both apoptosis and cell cycle arrest.[66,67]

CONCLUSONS

PAT guided approach for stringent control of CPP (μ) determining the higher huIFNα2b yield was successfully achieved using estimator based on real-time capacitance signal. This study also underscores the necessity of maintaining induction phase specific growth rate at a narrow range ($\mu = 0.015–0.04\ h^{-1}$) that would strongly influence the expression of huIFNα2b in glycoengineered *Pichia pastoris*. The design of a simple PID control strategy and setting optimal controller tuning parameter values, efficiently modulated the balance between the methanol uptake by the cells and subsequent channelling of its key metabolic activities (growth and protein production). A long-term stability of μ_{est} signal ($\approx$ 15 h) was achieved for very low and narrow range μ_{sp}, which can be attributed to the robustness of the controller. The feedback control of $\mu_{met} = 0.04\ h^{-1}$ resulted in an enhanced huIFNα2b (1483 mg L^{-1}) titer and specific productivity ($q_P = 0.457\ mg_{huIFN\alpha2b}\ g_{Biomass}^{-1}\ h^{-1}$) reported to date. The purified huIFNα2b was biologically active exhibiting antiproliferative activity in human breast cancer cell lines (T47D and MCF7). In an overall observation, this study demonstrates the potential of interpreting the real-time soft sensor information into CPP. In future this repertoire can be transformed to monitor a much more delicate biological system by applying various constraints and using advanced process control strategy. The simple and robust PAT based feedback control strategy proposed in this study forms a reliable process control approach for Quality by Design (QbD) as FDA mandate for industrial applications.

ACKNOWLEDGEMENTS

The authors gratefully acknowledge the financial assistance granted by the Department of Science and Technology – Science and Engineering Research Board, Governement of India under the project (grant no. SB/FTP/ETA-0448/2012). The authors kindly acknowledge Mr Nurul Islam, Technical Superintendent, Department of Biosciences and Bioengineering for his generous support. The authors are also grateful to Ms Nivedhitha Swaminathan, Research Student, Centre for Environment, IIT Guwahati for her technical assistance.

CONFLICT OF INTEREST

All the authors declare that they have no conflict of interest.

Supporting Information

Supporting information may be found in the online version of this article.

 © 2019 Society of Chemical Industry

REFERENCES

1 Ningrum R, Human interferon alpha-2b: a therapeutic protein for cancer treatment. *Scientifica* **2014**:970315 (2014).
2 Cereghino JL and Cregg JM, Heterologous protein expression in the methylotrophic yeast *Pichia pastoris*. *FEMS Microbiol Rev* **24**:45–66 (2000).
3 Macauley-Patrick S, Fazenda ML, McNeil B and Harvey LM, Heterologous protein production using the *Pichia pastoris* expression system. *Yeast* **22**:249–270 (2005).
4 Ahmad M, Hirz M, Pichler H and Schwab H, Protein expression in *Pichia pastoris*: recent achievements and perspectives for heterologous protein production. *Appl Microbiol Biotechnol* **98**:5301–5317 (2014).
5 Srikanth K, Yoganand KNR, Anand B and Senthilkumar S, Production of glycosylated human interferon alpha 2b in glycoengineered *Pichia pastoris*. Intellectual Property India 201731014991 (2018).
6 Katla S, Yoganand K, Hingane S, Kumar CR, Anand B and Sivaprakasam S, Novel glycosylated human interferon alpha 2b expressed in glycoengineered *Pichia pastoris* and its biological activity: N-linked glycoengineering approach. *Enzyme Microb Technol* **128**:49–58 (2019).
7 Rebnegger C, Graf AB, Valli M, Steiger MG, Gasser B, Maurer M *et al.*, In *Pichia pastoris*, growth rate regulates protein synthesis and secretion, mating and stress response. *Biotechnol J* **9**:511–525 (2014).
8 Damasceno LM, Huang C-J and Batt CA, Protein secretion in *Pichia pastoris* and advances in protein production. *Appl Microbiol Biotechnol* **93**:31–39 (2012).
9 Fazio A, Jewett MC, Daran-Lapujade P, Mustacchi R, Usaite R, Pronk JT *et al.*, Transcription factor control of growth rate dependent genes in *Saccharomyces cerevisiae*: a three factor design. *BMC Genomics* **9**:341 (2008).
10 Pinsach J, de Mas C and López-Santín J, A simple feedback control of *Escherichia coli* growth for recombinant aldolase production in fed-batch mode. *Biochem Eng J* **29**:235–242 (2006).
11 Schuler MM and Marison IW, Real-time monitoring and control of microbial bioprocesses with focus on the specific growth rate: current state and perspectives. *Appl Microbiol Biotechnol* **94**:1469–1482 (2012).
12 Food and Administration D, Guidance for industry, PAT-A Framework for Innovative Pharmaceutical Development, Manufacturing and Quality Assurance. Available: http://www fda gov/cder/guidance/published html (2004).
13 Dabros M, Dennewald D, Currie DJ, Lee MH, Todd RW, Marison IW *et al.*, Cole–Cole, linear and multivariate modeling of capacitance data for on-line monitoring of biomass. *Bioprocess Biosyst Eng* **32**:161–173 (2009).
14 Cole HE, Demont A and Marison IW, The application of dielectric spectroscopy and biocalorimetry for the monitoring of biomass in immobilized mammalian cell cultures. *Processes* **3**:384–405 (2015).
15 Davey CL, Davey HM, Kell DB and Todd RW, Introduction to the dielectric estimation of cellular biomass in real time, with special emphasis on measurements at high volume fractions. *Anal Biotechnol* **279**:155–161 (1993).
16 Kaiser C, Carvell J and Luttmann R, A sensitive, compact, *in situ* biomass measurement system controlling and monitoring microbial fermentations using radio-frequency impedance. *Bioprocess Int* **5**:52–56 (2007).
17 Maskow T, Röllich A, Fetzer I, Ackermann J-U and Harms H, On-line monitoring of lipid storage in yeasts using impedance spectroscopy. *J Biotechnol* **135**:64–70 (2008).
18 Rønnest NP, Stocks SM, Lantz AE and Gernaey KV, Introducing process analytical technology (PAT) in filamentous cultivation process development: comparison of advanced online sensors for biomass measurement. *J Ind Microbiol Biotechnol* **38**:1679–1690 (2011).
19 Cannizzaro C, Gügerli R, Marison I and von Stockar U, Online biomass monitoring of CHO perfusion culture with scanning dielectric spectroscopy. *Biotechnol Bioeng* **84**:597–610 (2003).
20 Schenk J, Balazs K, Jungo C, Urfer J, Wegmann C, Zocchi A *et al.*, Influence of specific growth rate on specific productivity and glycosylation of a recombinant avidin produced by a *Pichia pastoris* Mut+ strain. *Biotechnol Bioeng* **99**:368–377 (2008).
21 Zhang W, Smith LA, Plantz BA, Schlegel VL and Meagher MM, Design of methanol feed control in *Pichia pastoris* fermentations based upon a growth model. *Biotechnol Prog* **18**:1392–1399 (2002).
22 Pla IA, Damasceno LM, Vannelli T, Ritter G, Batt CA and Shuler ML, Evaluation of Mut+ and MutS *Pichia pastoris* phenotypes for high level extracellular scFv expression under feedback control of the methanol concentration. *Biotechnol Prog* **22**:881–888 (2006).
23 Ramon R, Feliu J, Cos O, Montesinos J, Berthet F and Valero F, Improving the monitoring of methanol concentration during high cell density fermentation of *Pichia pastoris*. *Biotechnol Lett* **26**:1447–1452 (2004).
24 Dabros M, Schuler MM and Marison IW, Simple control of specific growth rate in biotechnological fed-batch processes based on enhanced online measurements of biomass. *Bioprocess Biosyst Eng* **33**:1109–1118 (2010).
25 Ferreira A, Ataíde F, Von Stosch M, Dias J, Clemente J, Cunha A *et al.*, Application of adaptive DO-stat feeding control to *Pichia pastoris* X33 cultures expressing a single chain antibody fragment (scFv). *Bioprocess Biosyst Eng* **35**:1603–1614 (2012).
26 Goldfeld M, Christensen J, Pollard D, Gibson ER, Olesberg JT, Koerperick EJ *et al.*, Advanced near-infrared monitor for stable real-time measurement and control of *Pichia pastoris* bioprocesses. *Biotechnol Prog* **30**:749–759 (2014).
27 Schuler MM, Sivaprakasam S, Freeland B, Hama A, Hughes K-M and Marison IW, Investigation of the potential of biocalorimetry as a process analytical technology (PAT) tool for monitoring and control of Crabtree-negative yeast cultures. *Appl Microbiol Biotechnol* **93**:575–584 (2012).
28 Ehgartner D, Hartmann T, Heinzl S, Frank M, Veiter L, Kager J *et al.*, Controlling the specific growth rate via biomass trend regulation in filamentous fungi bioprocesses. *Chem Eng Sci* **172**:32–41 (2017).
29 Marison IW, Dabros M and Schuler MM, Beyond bioprocess monitoring and control. *Lab J* Available: https://www.laboratory-journal.com (2010) [1 February 2019].
30 Åström KJ and Hägglund T, The future of PID control. *IFAC Proc Vol* **33**:19–30 (2000).
31 Levisauskas D, Simutis R, Borvitz D and Lübbert A, Automatic control of the specific growth rate in fed-batch cultivation processes based on an exhaust gas analysis. *Bioproc Eng* **15**:145–150 (1996).
32 Caldwell J, Wang W and Zandstra PW, Proportional-integral-derivative (PID) control of secreted factors for blood stem cell culture. *PloS one* **10**:e0137392 (2015).
33 Katla S, Karmakar B, SRR T, Mohan N, Anand B, Pal U *et al.*, High level extracellular production of recombinant human interferon alpha 2b in glycoengineered *Pichia pastoris*: culture medium optimization, high cell density cultivation and biological characterization. *J Appl Microbiol* **126**:1438–1453 (2019).
34 Asami K, Takahashi K and Shirahige K, Progression of cell cycle monitored by dielectric spectroscopy and flow-cytometric analysis of DNA content. *Yeast* **16**:1359–1363 (2000).
35 Horta A, Silva A, Sargo C, Velez A, Gonzaga M, Giordano R *et al.*, A supervision and control tool based on artificial intelligence for high cell density cultivations. *Braz J Chem Eng* **31**:457–468 (2014).
36 Soons Z, Voogt J, Van Straten G and Van Boxtel A, Constant specific growth rate in fed-batch cultivation of *Bordetella pertussis* using adaptive control. *J Biotechnol* **125**:252–268 (2006).
37 Gnoth S, Jenzsch M, Simutis R and Lübbert A, Control of cultivation processes for recombinant protein production: a review. *Bioprocess Biosyst Eng* **31**:21–39 (2008).
38 Valentinotti S, Adaptive rejection of unstable disturbances: application to a fed-batch fermentation. PhD Thesis, École Polytechnique Fédérale de Lausanne (2001).
39 Howard R and Cooper D, A novel pattern-based approach for diagnostic controller performance monitoring. *Control Eng Pract* **18**:279–288 (2010).
40 Wechselberger P, Sagmeister P and Herwig C, Real-time estimation of biomass and specific growth rate in physiologically variable recombinant fed-batch processes. *Bioprocess Biosyst Eng* **36**:1205–1218 (2013).
41 Niu H, Daukandt M, Rodriguez C, Fickers P and Bogaerts P, Dynamic modeling of methylotrophic *Pichia pastoris* culture with exhaust gas analysis: from cellular metabolism to process simulation. *Chem Eng Sci* **87**:381–392 (2013).
42 Jahic M, Rotticci-Mulder J, Martinelle M, Hult K and Enfors S-O, Modeling of growth and energy metabolism of *Pichia pastoris* producing a fusion protein. *Bioprocess Biosyst Eng* **24**:385–393 (2002).
43 Zhang P, Zhang W, Zhou X, Bai P, Cregg JM and Zhang Y, Catabolite repression of Aox in *Pichia pastoris* is dependent on hexose transporter PpHxt1 and pexophagy. *Appl Environ Microbiol* **76**:6108–6118 (2010).

 © 2019 Society of Chemical Industry

44 Capone S, Horvat J, Herwig C and Spadiut O, Development of a mixed feed strategy for a recombinant *Pichia pastoris* strain producing with a de-repression promoter. *Microb Cell Fact* **14**:101 (2015).
45 Looser V, Bruhlmann B, Bumbak F, Stenger C, Costa M, Camattari A *et al.*, Cultivation strategies to enhance productivity of *Pichia pastoris*: a review. *Biotechnol Adv* **33**:1177–1193 (2015).
46 Katakura Y, Zhang W, Zhuang G, Omasa T, Kishimoto M, Goto Y *et al.*, Effect of methanol concentration on the production of human β2-glycoprotein I domain V by a recombinant *Pichia pastoris*: a simple system for the control of methanol concentration using a semiconductor gas sensor. *J Ferment Bioeng* **86**:482–487 (1998).
47 Wong HH, Kim YC, Lee SY and Chang HN, Effect of post-induction nutrient feeding strategies on the production of bioadhesive protein in *Escherichia coli*. *Biotechnol Bioeng* **60**:271–276 (1998).
48 Zhang W, Bevins MA, Plantz BA, Smith LA and Meagher MM, Modeling *Pichia pastoris* growth on methanol and optimizing the production of a recombinant protein, the heavy-chain fragment C of botulinum neurotoxin, serotype a. *Biotechnol Bioeng* **70**:1–8 (2000).
49 Zhang B, Li B, Chen D, Zong J, Sun F, Qu H *et al.*, Transcriptional regulation of aerobic metabolism in *Pichia pastoris* fermentation. *PloS one* **11**:e0161502 (2016).
50 Xie J, Yang R, Zhou Q, Du P, Gan R and Ye Q, Efficiencies of growth and angiostatin expression in cultures of *Pichia pastoris* fed with mixed carbon sources. *Chem Biochem Eng Q* **27**:235–244 (2013).
51 Trinh L, Phue J and Shiloach J, Effect of methanol feeding strategies on production and yield of recombinant mouse endostatin from *Pichia pastoris*. *Biotechnol Bioeng* **82**:438–444 (2003).
52 Looser V, Lüthy D, Straumann M, Hecht K, Melzoch K and Kovar K, Effects of glycerol supply and specific growth rate on methanol-free production of CALB by *P. pastoris*: functional characterisation of a novel promoter. *Appl Microbiol Biotechnol* **101**:3163–3176 (2017).
53 Jacobs PP, Inan M, Festjens N, Haustraete J, Van Hecke A, Contreras R *et al.*, Fed-batch fermentation of GM-CSF-producing glycoengineered *Pichia pastoris* under controlled specific growth rate. *Microb Cell Fact* **9**:93 (2010).
54 Wu D, Chu J, Hao Y-Y, Wang Y-H, Zhuang Y-P and Zhang S-L, High efficient production of recombinant human consensus interferon mutant in high cell density culture of *Pichia pastoris* using two phases methanol control. *Process Biochem* **46**:1663–1669 (2011).
55 Potgieter TI, Kersey SD, Mallem MR, Nylen AC and d'Anjou M, Antibody expression kinetics in glycoengineered *Pichia pastoris*. *Biotechnol Bioeng* **106**:918–927 (2010).
56 Smith ET, Perry ET, Sears MB and Johnson DA, Expression of recombinant human mast cell chymase with Asn-linked glycans in glycoengineered *Pichia pastoris*. *Protein Expr Purif* **102**:69–75 (2014).
57 Tuite M, Dobson M, Roberts N, King R, Burke D, Kingsman S *et al.*, Regulated high efficiency expression of human interferon-alpha in *Saccharomyces cerevisiae*. *EMBO J* **1**:603–608 (1982).
58 Shi L, Wang D, Chan W and Cheng L, Efficient expression and purification of human interferon alpha 2b in the methylotrophic yeast. *Pichia Pastoris Protein Expr Purif* **54**:220–226 (2007).
59 Ghosalkar A, Sahai V and Srivastava A, Secretory expression of interferon-alpha 2b in recombinant *Pichia pastoris* using three different secretion signals. *Protein Expr Purif* **60**:103–109 (2008).
60 Ayed A, Rabhi I, Dellagi K and Kallel H, High level production and purification of human interferon α2b in high cell density culture of *Pichia pastoris*. *Enzyme Microb Technol* **42**:173–180 (2008).
61 Salunkhe S, Soorapaneni S, Prasad KS, Raiker VA and Padmanabhan S, Strategies to maximize expression of rightly processed human interferon α2b in *Pichia pastoris*. *Protein Expr Purif* **71**:139–146 (2010).
62 Gasmi N, Ayed A, Ammar BB, Zrigui R, Nicaud J-M and Kallel H, Development of a cultivation process for the enhancement of human interferon alpha 2b production in the oleaginous yeast, *Yarrowia lipolytica*. *Microb Cell Fact* **10**:90 (2011).
63 Ningrum RA, Wisnuwardhani PH, Santoso A and Herawati N, Antiproliferative activity of recombinant human interferon alpha 2B on estrogen positive human breast cancer MCF-7 cell line. *Indonesian J Pharm* **26**:86 (2015).
64 Levin D, Harari D and Schreiber G, Stochastic receptor expression determines cell fate upon interferon treatment. *Mol Cell Biol: MCB* **31**:05251–05211 (2011).
65 Ningrum RA, Rahmatika DE, Retnoningrum DS, Wangsaatmadja AH, Sumirtapura YC and Rachmawati H, Development of novel interferon alpha 2b muteins and study the pharmacokinetic and biodistribution profiles in animal model. *J Biomed Sci Eng* **5**:104–112 (2012).
66 Kalie E, Jaitin DA, Abramovich R and Schreiber G, An interferon α2 mutant optimized by phage display for IFNAR1 binding confers specifically enhanced antitumor activities. *J Biol Chem* **282**:11602–11611 (2007).
67 Roos G, Leanderson T and Lundgren E, Interferon-induced cell cycle changes in human hematopoietic cell lines and fresh leukemic cells. *Cancer Res* **44**:2358–2362 (1984).

 © 2019 Society of Chemical Industry